

Headcut Prevention



Patrick Ndolo Goy, Youngjai Jung

April 11, 2013

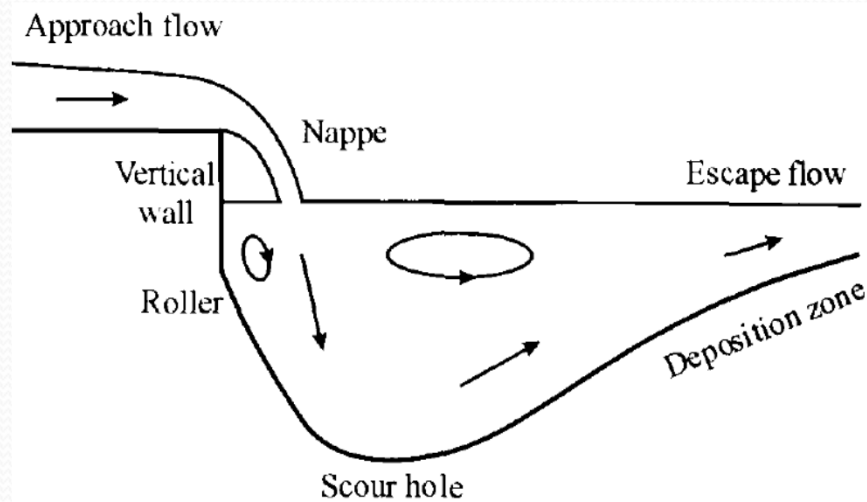


Objective

- Objective
 - study the Headcut characteristics in the natural river
 - search the stabilization method
- Contents
 - Physical process of Headcut
 - Governing equations
 - Numerical model and Lab experiment Study
 - Field Structure to prevent headcut

What is Headcut?

- Ddowncutting of streambed in upstream direction
- Near-vertical drop or discontinuity on the channel bed of stream, rill or gully, at which a free overfall flow often **OCCURS**



Schematic diagram of headcut

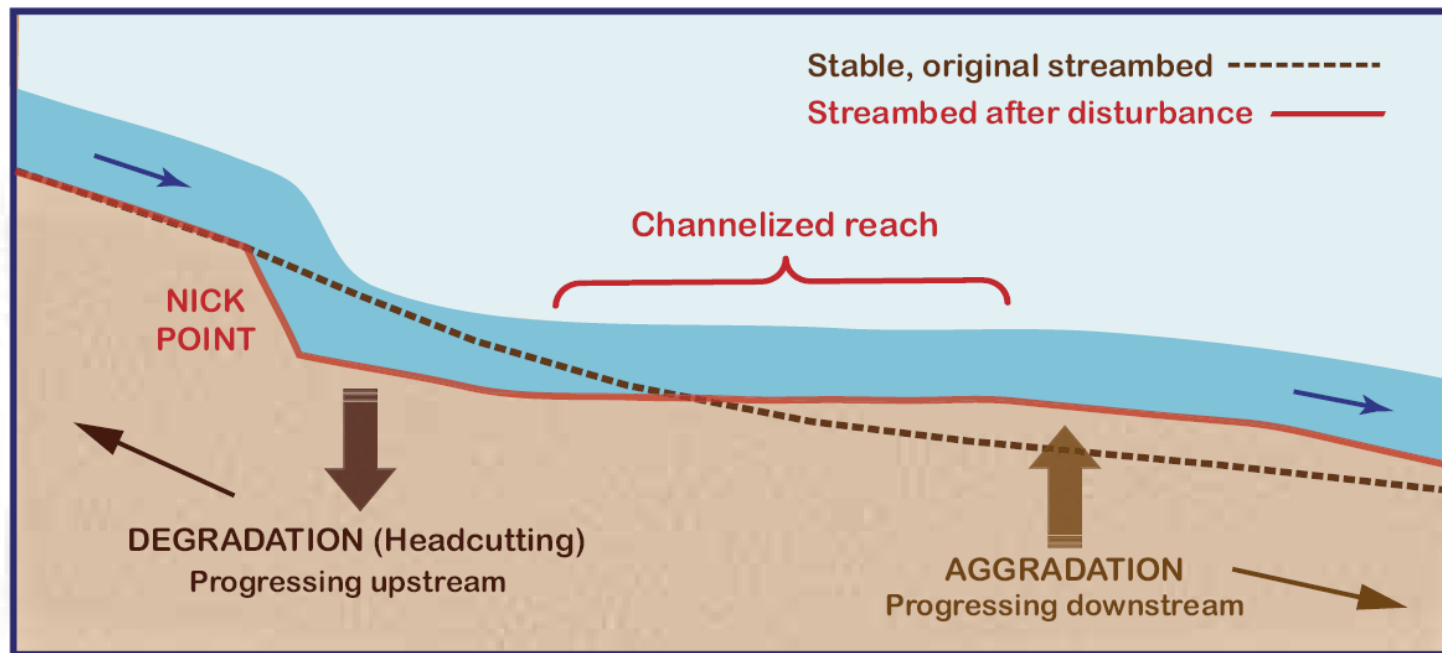
(W. Wu and S. S. Wang, 2005)



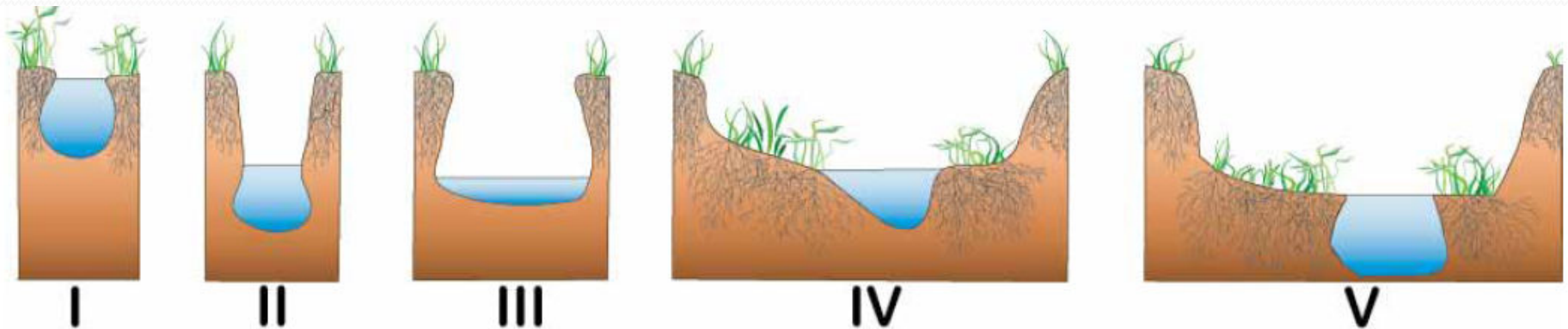
Headcut in Pawnee Buttes
(Photo by Youngjai)

Physical Process

- Increased flow velocity over a headcut continues erosion at the head cut depth in the upstream direction manifesting the head cut feature head ward



Physical Process



- I. A properly shaped stream in **equilibrium** and connected to its floodplain prior to disturbance.
 II. **Channel incision** from ditching or by a headcut originating in a channelized reach due to increased slope and flow.
 III. **Channel widening** as the channel begins to meander again.
 IV. A more properly shaped stream as it evolves to re-establish equilibrium and rebuild a new floodplain.
 V. A new, properly shaped channel in equilibrium with a lowered floodplain.

I Stable

$$h < h_c$$

II Headcut

$$h > h_c$$

III Widening

$$h > h_c$$

IV Stabilizing

$$h = h_c$$

V Stable

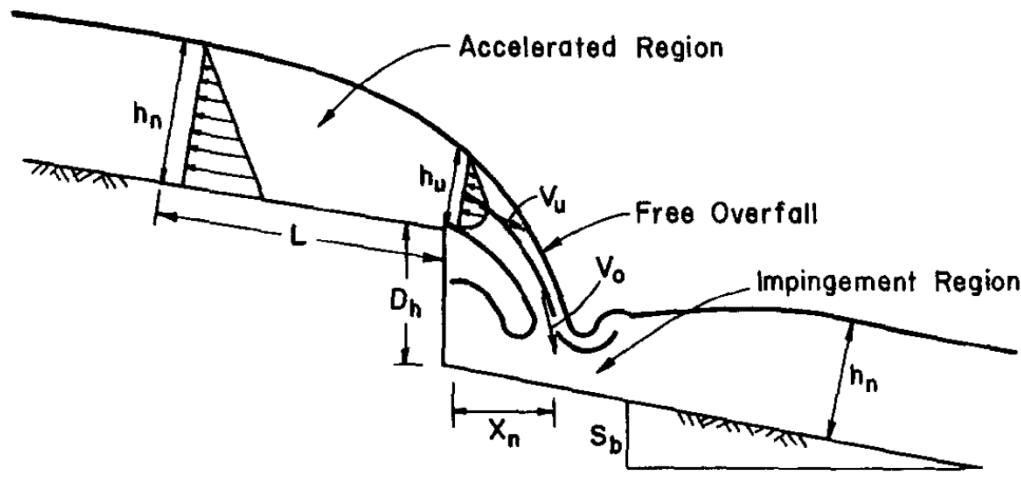
$$h < h_c$$

h : bank flow depth

h_c : critical bank flow depth

Governing Equations

- Two dimensional flow over a headcut of drop height D_h in a wide rectangular channel of constant slope S .



Initial Headcut Hydraulics

(Source: O. R. Stein and P. Y. Julien, 1993)

- Steady flow of unit discharge q , uniform at a normal flow depth h_n
- A nearly hydrostatic pressure distribution upstream from the headcut
- Pressure distribution less than hydrostatic at the brink
- Flow to accelerate through a distance $L \cong 2$ to 4 times h_n
- Depth gradually decreases from normal flow h_n to depth h_u at the brink
- Average flow velocity at the brink V_u
- Water falls freely through a drop height D_h , accelerates from V_u at the brink to V_o when entering the impingement region
- Jet impinges on the downstream water surface at a distance X_n downstream from the headcut face.

Governing Equations

- Accelerated-Flow Region

- The upstream h_n and $V_n = q/h_n$ function of slope S and Reynolds number R (Julien and Simons 1985) :

$h_n = aS^bR^c$, a , b and c are listed in the table below

Type of flow	a	b	c
Laminar (k =constant)	$(k\nu^2/8g)^{1/3}$	-1/3	1/3
Turbulent, smooth boundary	$(0.22\nu^2/8g)^{1/3}$	-1/3	7/12
Turbulent (n =constant)	$(n\nu)^{6/10}$	-3/10	6/10
Turbulent (f =constant)	$(f\nu^2/8g)^{1/3}$	-1/3	2/3

k = resistance parameter for laminar flow
 n = Manning resistance coefficient
 f = Darcy-Weisbach friction factor
 ν = kinematic viscosity
 g = gravitational acceleration

(Source: O. R. Stein and P. Y. Julien, 1993)

Governing Equations

- Accelerated-Flow Region

- The flow depth h_u and velocity V_u at the brink: (from Rouse 1936, 1937; Delleur et al. 1956; Rajaratnam and Muralidhar 1968):

$$\frac{V_n}{V_u} = \frac{h_u}{h_n} = \frac{F^2}{F^2 + 0.4}$$

F = upstream Froude number
 h_u = flow depth at the brink
 V_u = velocity at the brink

- The shear stress at the brink: $\tau_u = C_u \rho V_u^2$
- The normal shear stress: $\tau_n = C_u \rho V_u^2$
- The ratio of τ_u to τ_n is:

$$\frac{\tau_u}{\tau_n} = \frac{C_u \rho V_u^2}{C_u \rho V_n^2} = \left(1 + \frac{0.4}{F^2}\right)^2$$

C_u = upstream friction coefficient (it is assumed remain constant)
 ρ = fluid density

Governing Equations

- Free Overall Region

- The free-falling nappe is accelerating from the brink to the impingement point
- D_h is the initial drop height of the headcut
- Velocity increases from V_u at the brink to V_o at the tailwater impingement point X_n
- From conservation of energy equation for free-falling fluid and assuming a small tailwater depth:

$$V_o = \sqrt{V_u^2 + 2gD_h} = V_n \left(1 + \frac{0.4}{F^2} \right) \sqrt{1 + \frac{2gD_h}{V_u^2}}$$

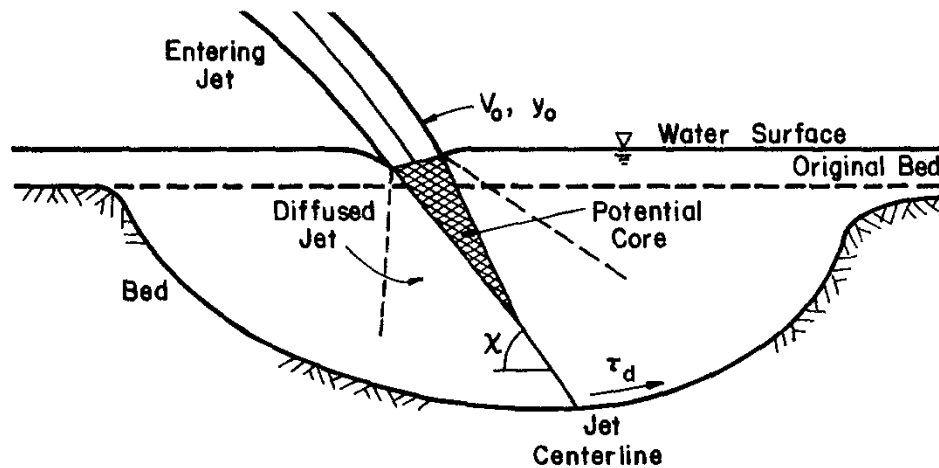
And

$$\frac{X_n}{D_h} = V_u \sqrt{\frac{2}{gD_h}} = \sqrt{2} \sqrt{\frac{h_n}{D_h} \left(\frac{F^2 + 0.4}{F} \right)}$$

- V_o and X_n determine the velocity and location of the impact point of the jet entering the impinging region. (Source: O. R. Stein and P. Y. Julien, 1993)

Governing Equations

- Impingement Region



Hydraulics of Impingement Region

- At the impact with the water surface, the jet has an initial thickness y_0 , average velocity V_0 and impact angle χ
- The maximum bed shear stress in the impingement region occurs while the bed is within the jet potential core in which the maximum velocity remains V_0
- The maximum shear stress in the impingement region:

$$\tau_d = C_d \rho V_0^2$$

$$\frac{\tau_d}{\tau_n} = \frac{C_d \rho V_0^2}{C_u \rho V_n^2} = \frac{C_d}{C_u} \left[\left(1 + \frac{0.4}{F^2} \right) + \left(\frac{2}{F^2} \frac{Dh}{h_n} \right) \right]$$

$$\frac{\tau_d}{\tau_u} = \frac{C_d}{C_u} \left[1 + \frac{2Dh}{h_n} \left(\frac{F}{F^2 + 0.4} \right)^2 \right]$$

Stein (1990) and Stein et al. (1993)

(Source: O. R. Stein and P. Y. Julien, 1993)

Numerical Model

HEADCUT MIGRATION (W. Wu and S. S. Y. Wang, 2005)

- **Hydrodynamic Model**

- Flow simulated using the model developed by Wu et al. (2000), which solves the Reynolds-averaged Navier-Stokes equations;
- The pressure is calculated by the SIMPLE (Semi-Implicit Method for Pressure Linked Equations) algorithm;
- The convection terms are discretized by the HLP (Hybrid Linear/Parabolic Approximation) scheme (Zhu, 1992);
- The effect of turbulence is determined with the standard $k - \varepsilon$ turbulence model;
- The effect of bed and bank roughness is taken into account with a wall-function approach;
- The water surface is calculated by a Poisson equation derived from the depth-averaged 2-D momentum equations for shallow open-channel flow;
- The boundaries vary with time due to the free-surface change, bed deformation and headcut migration;
- An adaptive-grid technique in the longitudinal direction is implemented to capture the moving boundary due to the headcut migration, combined with the original adaptive-grid technique in the vertical direction to trace the water surface change and bed deformation;
- At each time step (iteration step), the computational grid is adapted after the calculations of water level, bed deformation and headcut migration.

Numerical Model

HEADCUT MIGRATION (W. Wu and S. S. Y. Wang, 2005)

• Sediment Transport Model

- The suspended-load transport is simulated by solving the general convection-diffusion equation with the finite volume method;
- The bed-load transport is calculated by a non-equilibrium transport model;
- The bed deformation is determined by the mass-balance equation integrated over the water depth (Wu et al., 2000);
- The bed-load transport capacity and the equilibrium near-bed suspended-load concentration required in the model are calculated by van Rijn's (1984) methods modified by Wu et al (1999):

$$q_{b*} = 0.053 \left(\frac{\rho_s - \rho}{\rho} g \right)^{0.5} \frac{d^{1.5}}{D_*^{0.3}} \left(\frac{\tau_e}{\tau_c} - 1 \right)^{2.1}$$

$$c_{b*} = 0.015 \frac{d}{b D_*^{0.3}} \left(\frac{\tau_e}{\tau_c} - 1 \right)^{1.5}$$

$$D_* = d [g(\rho_s - \rho) / \rho \nu^2]^{1/3}$$

$$\tau_c = K_p K_d K_s \tau_{co}$$

q_{b*} = the equilibrium transport rate of bed load
 c_{b*} = the equilibrium concentration of suspended load at the reference level
 b = the distance from the reference level to the bed
 D_* = the non-dimensional particle size
 g = the gravitational acceleration
 ρ_s and ρ = the densities of sediment and water
 d = the sediment size
 ν = the kinematic viscosity
 τ_c = the critical shear stress for sediment incipient motion in the rapidly-varying flow
 τ_{co} = the critical shear stress for sediment incipient motion from Shields curve

Numerical Model

HEADCUT MIGRATION (W. Wu and S. S. Y. Wang, 2005)

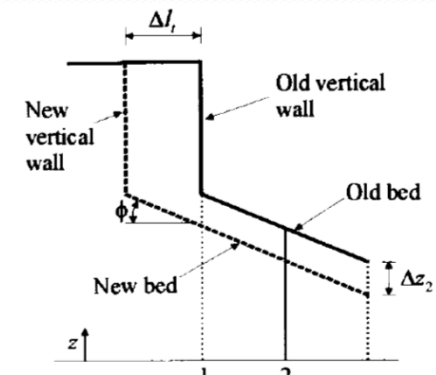
• Headcut Migration Model

- 3 modes of erosion occurring at the headcut:
 - ❑ First mode: surficial erosion along the vertical headwall due to the hydraulic shear of the flow
 - ❑ Second mode: toe erosion due to the scour hole development in the plunge pool
 - ❑ Third mode: mass failure occurs after the headwall exceeds the criterion of stability due to the development of the surficial erosion (first mode) and toe erosion (second mode)
- The erosion rate on the vertical headwall due to the hydraulic shear of flow is determined with the following equation.

$$\frac{dl}{dt} = \begin{cases} 0.0000625 \frac{\tau_{vm}}{M} \\ 0.00977 - 0.00238 \frac{\tau_{vm}}{M} + 0.000153 \left(\frac{\tau_{vm}}{M} \right)^2 \end{cases}$$

$$\begin{aligned} \frac{\tau_{vm}}{M} &< 8 \\ \frac{\tau_{vm}}{M} &\geq 8 \end{aligned}$$

M = material-dependent parameter
 τ_{vm} = the maximum shear stress on the headwall



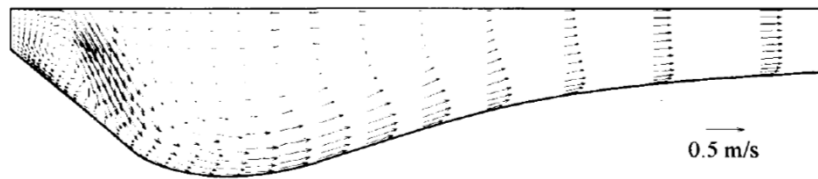
Numerical Model

HEADCUT MIGRATION (W. Wu and S. S. Y. Wang, 2005)

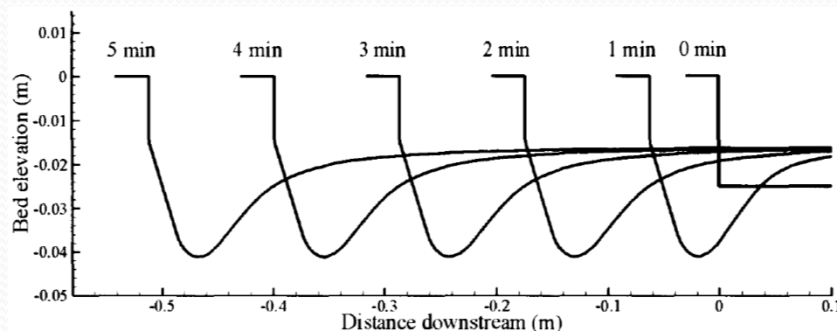
• Headcut Migration Model

- In each time step Δt , this equation gives the erosion length Δl_s on the vertical headwall
- The bed change Δz_2 in a time step Δt is calculated in accordance with the sediment transport model above
- The retreat length of the headcut due to the scour toe is: $\Delta l_t = \Delta z_2 / \tan \phi$
- The real migration length of a headcut in the time step Δt is the maximum of Δl_s and Δl_t .

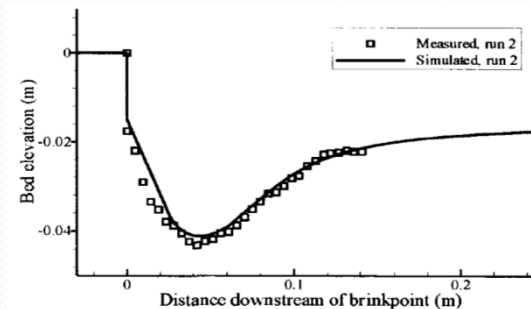
• Model Testing against Experimental Data



Calculated steady-state velocity vectors below a headcut for Bennett et al.'s (2000) experiments (Run 2)



Calculated headcut migration process for Bennett et al.'s (2000) experiments (Run 2)



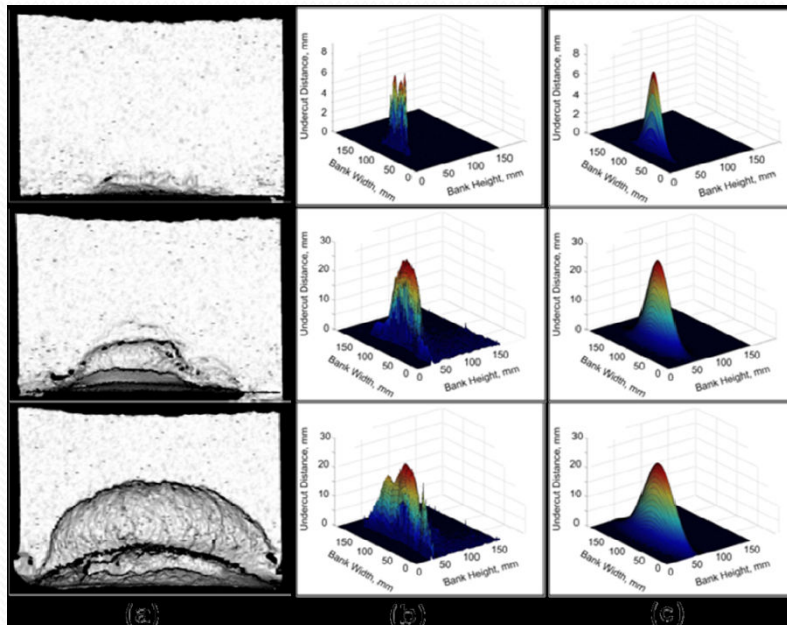
Steady-state scour hole profile for Bennett et al.'s (2000) experiments

(Source: W.Wu and S. S. Y. Wang, Empirical-Numerical Analysis of Headcut migration, International Journal of Sediment Research, Vol. 20, No. 3, 2005, pp. 233-243)

Lab. Experiment

Geometric Headcut Relationships for Predicting Seepage Erosion Undercutting by M.L. Chu-Agor, G.A. Fox, and G.V. Wilson

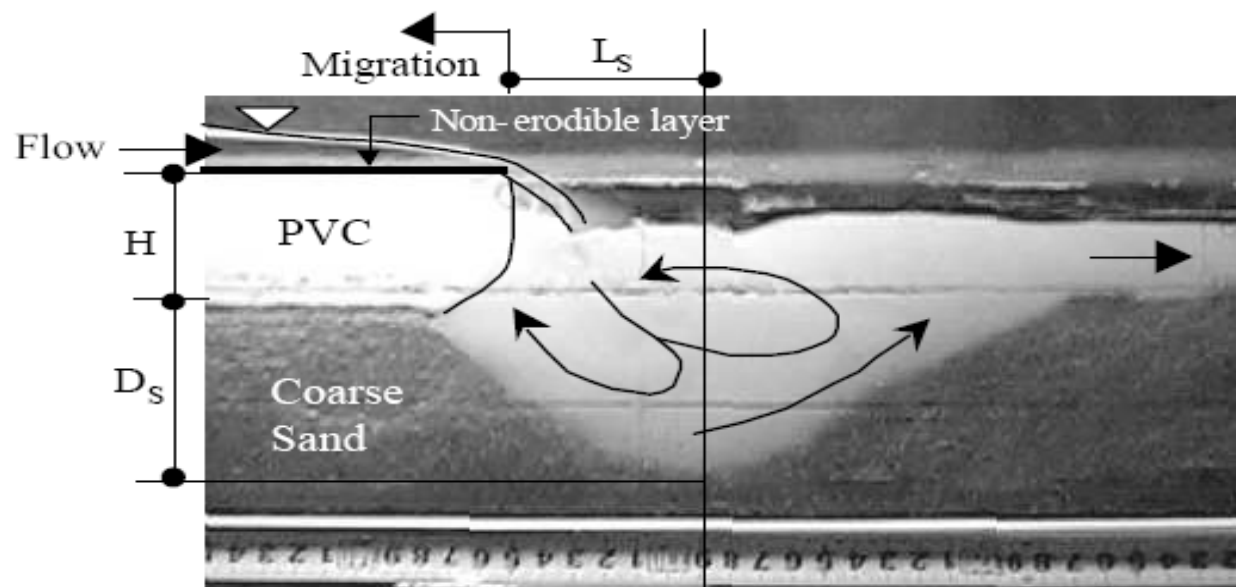
- Using a 3D Gaussian function, relationship between the eroded volume per bank face area and the amplitude of the headcut was derived
- The ground water velocity can be used with the derived sediment transport function to predict the dimensions of the headcut and the geometry of the undercut which enables the prediction of the impact of seepage erosion undercutting on hill slope stability.



Lab. Experiment

Headcut Erosion Process in Stratified Soil Layer of Flood Plain by Ashis Kumar Dey, Tetsuro Tsujimoto, and Tadanori Kitamura

- Headcut migration process in stratified non-cohesive soil was investigated
- During migration, a steady state condition was achieved where the plunge pool geometry and rate of migration remained unchanged.
- The plunge pool morphology remained unchanged with time for a given flow discharge
- The migration speed increased with flow discharge and headcut height





Negative Effect of Headcut

- For Nature
 - Base level drop: Earthquakes or tectonic processes
 - Ground water sapping: Topographically caused ground water concentration or piping
 - Change in sediment regime: fire induced runoff, draught, flooding
- Human Induced:
 - Increased sediment input to a reach from agriculture harvest
 - Decreased sediment input to a reach due to stream bank armoring
 - Increased runoff from urban areas
 - Change in output elevation/water level (i.e. reservoirs)

Headcut Prevention

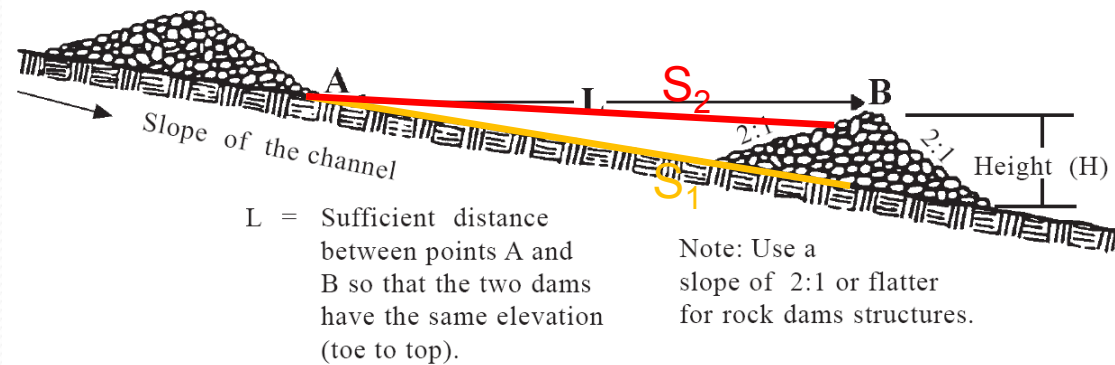
Headcuts can be prevented by maintaining the natural watershed condition with regard to flow, sediment and slope

- Straightening channels (ΔS_o)
- Gravel mining (ΔD_{50})
- Land Use change (ΔQ & D_{50})
 - Farming
 - Road construction
 - Grazing
 - Mining
 - Urbanization

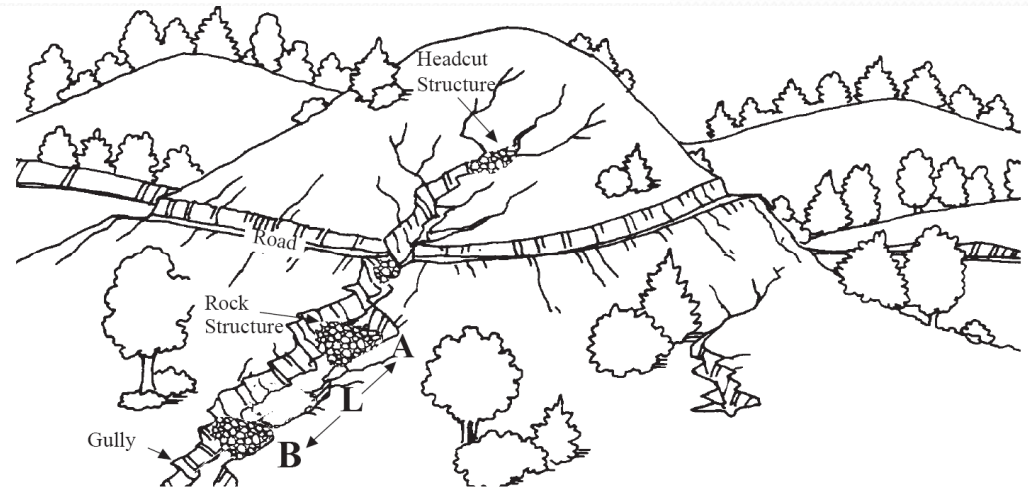


Headcut Control Structure

Existing headcuts can be controlled with hydraulic structures placed either above or below the headcut. The control structure causes the aggradation of sediment above it and decreases the bed slope



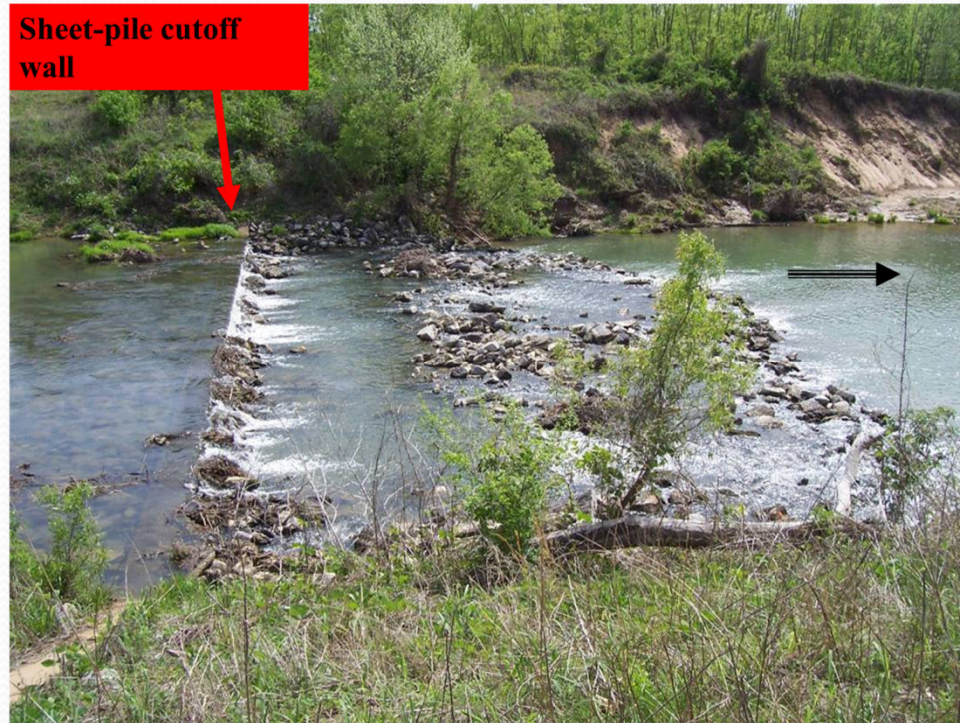
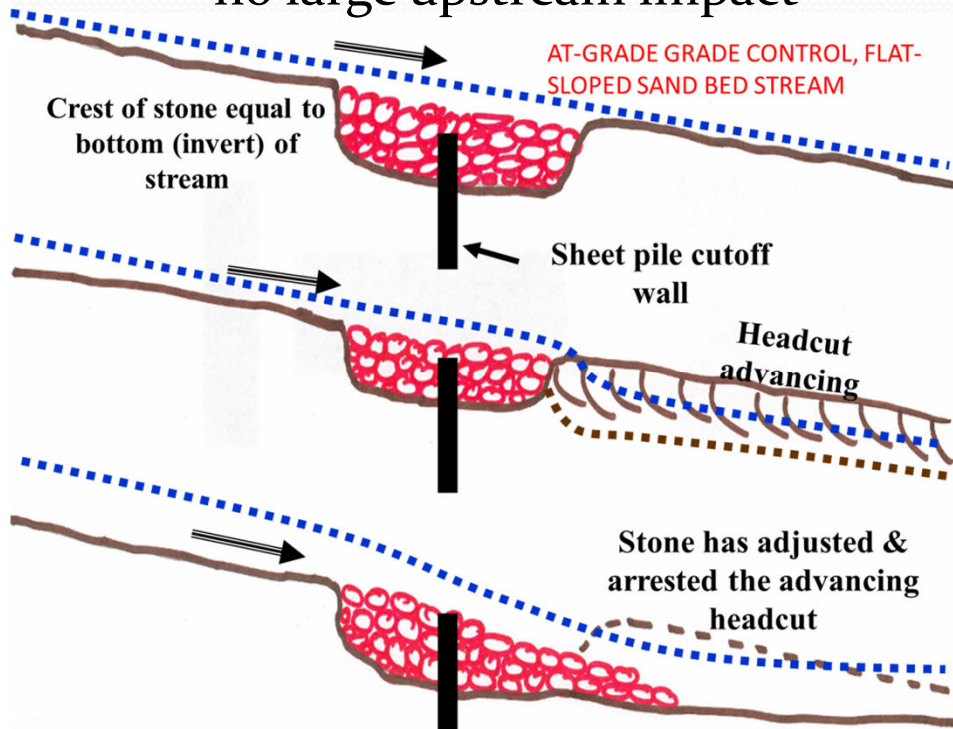
- Grade Control Structures
- Rock Mulch
- Rock Gabion
- Cheek Structures



Grade Control Structure

Bed Control Structure provides

- a hard point to resist erosion
- reduction in bed slope, energy slope
- Reduce bed scour and energy gradient
- no large upstream impact

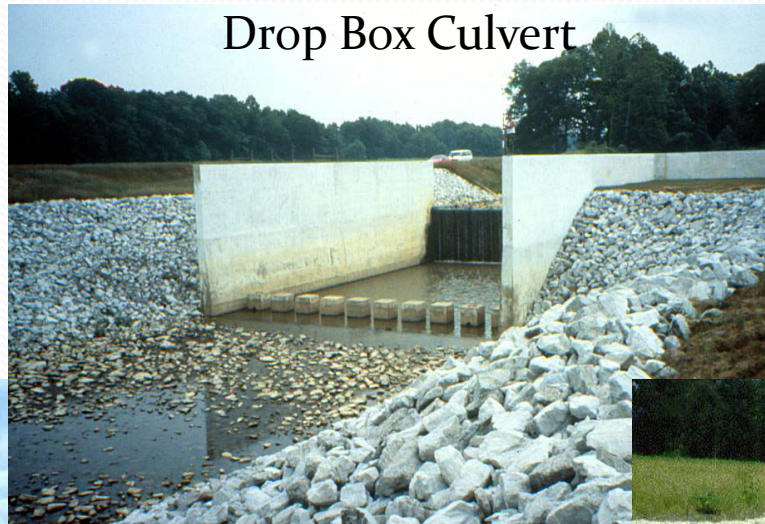


Grade Control Structure on Hickahalla Creek near Senatobia

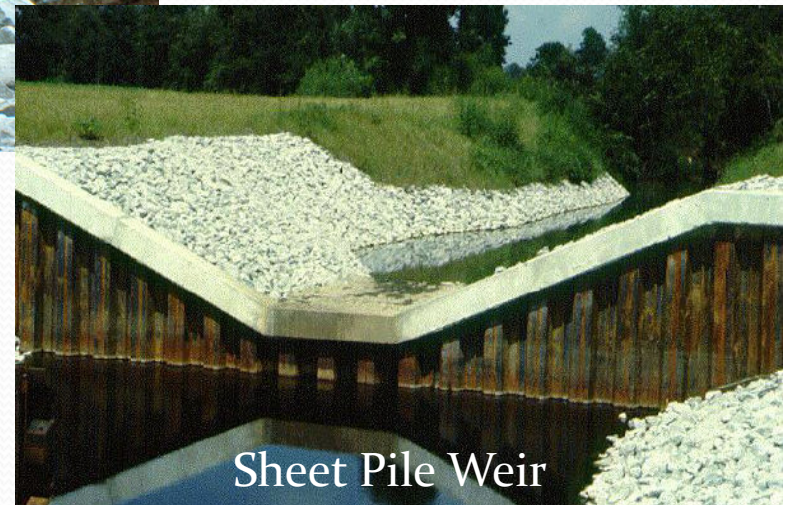
Grade Control Structures

In choosing the type of structure, frequency and number of structures and other criteria such as cost, material availability, environmental impacts, and risk must be seriously considered

Drop Box Culvert



Baffle Shoot Drop



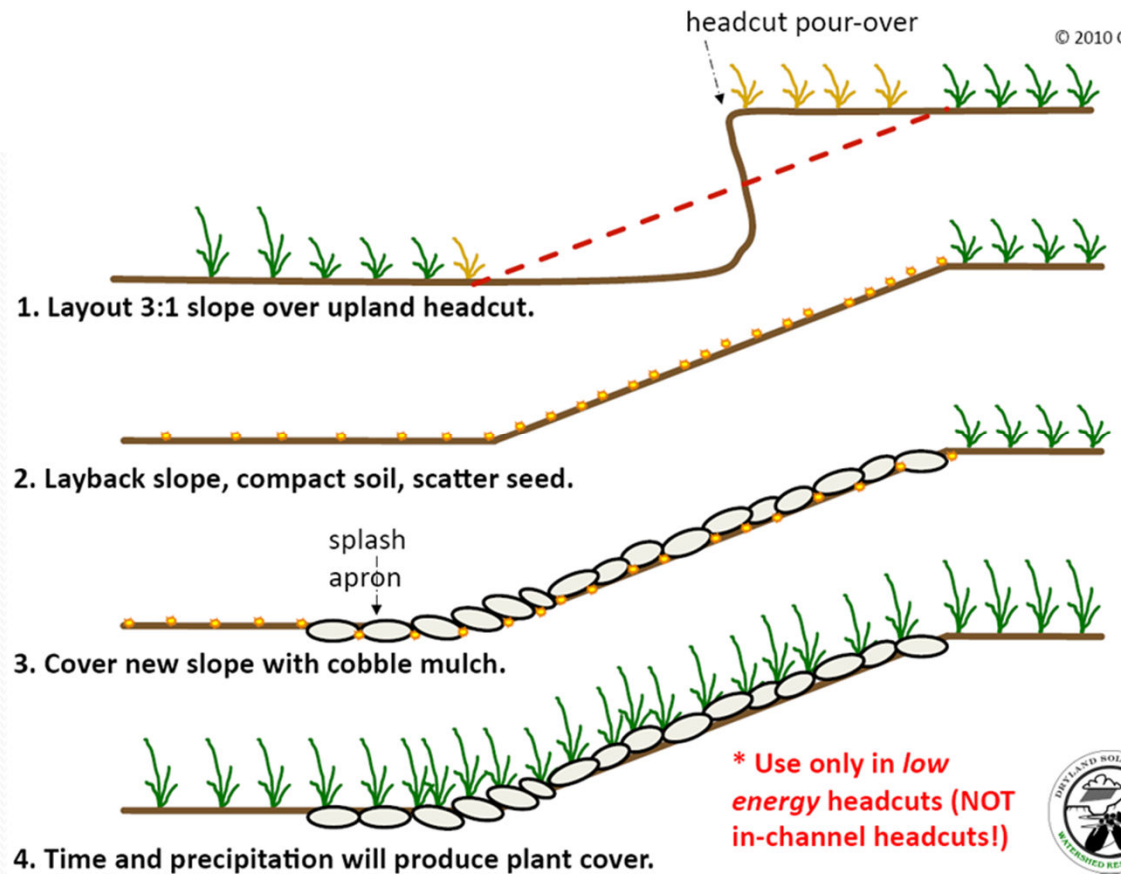
Sheet Pile Weir

Rock Mulch

A headcut control structure has been laid back to a stable angle of repose, and then covered with a single layer of rock mulch.

It serves to

- Slow runoff
- Increase soil moisture
- Recruit vegetation
- Prevent headcut from migrating further up slope



Rock Mulch (con.)

Rock Mulch Rundowns are only to be used on low energy headcuts, like those found in upland rills and gullies with small catchment areas, and where sheet-flow collects and enters a channel

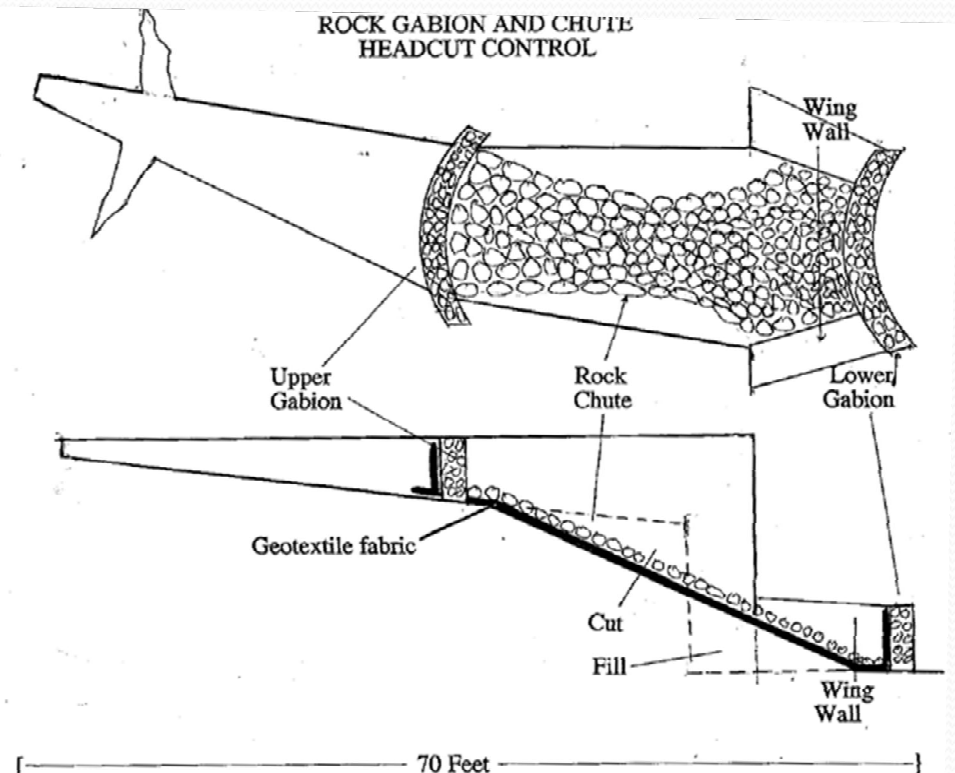


Rock Gabion

The rock-gabion drop structures are applied on a side headcut and gully on the Tillman County large gully system.

A gabion is a rock-filled fence-like structure intended to

- absorb the force of flowing water
- allowing sediment to settle out
- stabilize cut-banks



Cheek Structure

Left - Logs being used to build gully stabilization structures in a fire damaged area. Physical or vegetative dams may be used to control sediment and stabilize gullies

Right - Construct debris retention and gully control structures with a notched wier to keep flow over the middle of the structure, add scour protection at the outlet of each structure

